Impacts of the hydroxyls crosslinking on lignin softening and pyrolysis via in situ 1H NMR, rheology, DRIFT and SPI-MS

Zhiguo Dong, Anthony Dufour, Richard Laine, Sebastien Leclerc, Liangyuan Jia, Yingquan Chen, Xianhua Wang, Hanping Chen, Haiping Yang

▶ **To cite this version:**

Zhiguo Dong, Anthony Dufour, Richard Laine, Sebastien Leclerc, Liangyuan Jia, et al.. Impacts of the hydroxyls crosslinking on lignin softening and pyrolysis via in situ 1H NMR, rheology, DRIFT and SPI-MS. Fuel Processing Technology, 2022, 236, pp.107390. 10.1016/j.fuproc.2022.107390 . hal-03736217

HAL Id: hal-03736217

https://hal.univ-lorraine.fr/hal-03736217

Submitted on 22 Jul 2022

HAL is a multi-disciplinary open access archive for the deposit and dissemination of scientific research documents, whether they are published or not. The documents may come from teaching and research institutions in France or abroad, or from public or private research centers.

L'archive ouverte pluridisciplinaire **HAL**, est destinée au dépôt et à la diffusion de documents scientifiques de niveau recherche, publiés ou non, émanant des établissements d'enseignement et de recherche français ou étrangers, des laboratoires publics ou privés.

Impacts of the hydroxyls crosslinking on lignin softening and pyrolysis via *in situ* ^{1}H NMR, rheology, DRIFT and SPI-MS

Zhiguo Dong[a,b], *Anthony Dufour*[b*], *Richard Laine*[b], *Sebastien Leclerc*[c], *Liangyuan Jia*[d], *Yingquan Chen*[a], *Xianhua Wang*[a], *Hanping Chen*[a], *Haiping Yang*[a*]

[a] State Key Laboratory of Coal Combustion, School of Energy and Power Engineering, Huazhong University of Science and Technology, Wuhan, 430074, China

[b] LRGP, CNRS, Université de Lorraine, ENSIC, 1 rue Grandville 54000 Nancy, France

[c] LEMTA (UMR 7563)–CNRS–Universtité de Lorraine, Vandoeuvre-lès-Nancy, France

[d] School of Chemistry and Chemical Engineering, Hefei University of Technology, Hefei, Anhui 230009, China

Abstracts:

The softening and foaming of lignin during pyrolysis are the main obstacles to the scale-up of lignin pyrolysis systems. In this study, the mechanism of borate crosslinking on lignin softening and pyrolysis process was investigated by combining *in-situ* physical and chemical techniques. First, the mobile protons and visco-elastic modulus during lignin pyrolysis were quantitatively analyzed by *in-situ* high temperature ^{1}H NMR and rheology. It was found that the maximum content of mobile protons during the pyrolysis of raw lignin is around 90%. Hydroxyl crosslinking greatly inhibits the formation of mobile protons. The raw lignin produces a soft material from about 150 ℃ and starts to form a more rigid material from 200 ℃. At 210 ℃ ~ 330 ℃, mobile liquid-like intermediates are entrapped in the rigid char, forming “cavities”. With the addition of boron, the viscoelasticity tends to be stable and mainly elastic. Then, *in-situ* diffuse reflectance infrared Fourier transform spectroscopy and single photoionization time-of-flight mass spectrometry were used to characterize the

evolution of functional groups and volatiles. It was found that the shielding of hydroxyl groups by borate inhibits the decomposition of lignin but improves the selectivity to phenols, and more oxygenated groups remain in the char.

Keywords: Lignin; Softening; Pyrolysis; Borate; Char

1. Introduction

Lignin resource utilization is of great significance to the construction of green and low-carbon energy structures. Pyrolysis is an attractive technology to convert lignin into high-value chemicals and fuels[1]. However, the adverse effects of lignin softening and foaming on the system mass transfer and product properties are an important issue[2].

Several studies have attempted to reveal the origin of lignin softening and its influence on pyrolysis. Shrestha et al.[3] found that the softening of lignin is due to glass phase transition overlapped with the scission of covalent bonds, giving more low molecular weight mobile species. Tiarks et al.[4] observed that lignin underwent the whole process of melting, agglomeration, ejection, and volatilization using imaging, and pointed out that liquid coalescence was the main reason for the droplet thermal ejection. Zhou et al.[5] has even found that thermal ejection of liquid intermediates was the main way to form pyrolytic lignin. Dufour et al.[6] pointed out that isolated lignin was more mobile than in native lignocellulosic biomass because more interactions between polymers occur in the natural biomass network. Kubo et al.[7] studied the non-covalent hydrogen bonding in lignin and found that intermolecular hydrogen bonds formed between bisphenol and phenol moieties could reduce the thermal mobility of lignin, but they also found that phenolic hydroxyl groups are more difficult to form hydrogen bonds than aliphatic hydroxyl groups.

Therefore, properly strengthening molecular interactions, such as cross-linking, would likely improve lignin pyrolysis.

Xin et al.[8] reported that torrefaction pretreatment of lignin could promote the crosslinking and condensation of lignin and then prevent the bed agglomeration during pyrolysis. Ghysels et al.[9] mixed 20% calcium hydroxide with lignin, and found that calcium hydroxide could form bridging bonds between the two hydroxyl groups of lignin, which inhibited the agglomeration of char with more monomers produced. Magnesium hydroxide and calcium carbonate have also been found to have a similar action mechanism on lignin[10, 11]. However, the crosslinking efficiency of these modification methods is lower. Boron compounds (boric acid or borates), as a kind of highly efficient hydroxyl crosslinking agents, have been used to speed up the stabilization of lignin-based carbon fibers[12]. Our previous study also found that boron compounds could inhibit the char agglomeration during the pyrolysis of lignin, and boron-doped carbon nanospheres were obtained[13]. However, how the interactions between borate and lignin may improve the softening and pyrolysis of lignin is poorly understood.

In situ non-invasive analysis is very important to reveal the pyrolysis mechanism of biomass. For example, Dai et al.[14] studied the pyrolysis mechanism of hemicellulose by *in situ* diffuse reflectance infrared Fourier transform spectroscopy (DRIFT) and TG-PIMS. However, these methods are not tailored to analyze the physical properties of biomass during pyrolysis. In recent years, in-situ high temperature ^{1}H NMR and rheology have been used to analyze the matrix mobility and rheological properties during biomass pyrolysis[15]. Therefore, it is necessary to combine these methods to reveal the physical-chemical mechanism of lignin pyrolysis.

Hence, in this study, the mechanism of borate crosslinking on lignin softening and pyrolysis was explored. *In situ* ^{1}H NMR was used for the quantitative analysis of mobile protons during lignin pyrolysis, while rheology was used to study the viscoelastic properties of lignin undergoing thermal conversion. In addition, DRIFT spectroscopy was used to investigate the changes in functional groups during lignin pyrolysis, and a micro-fixed bed reactor combined with single photoionization time-of-flight mass spectrometry (SPI-TOFMS) was used to monitor the release properties of volatiles.

2. Materials and methods

2.1. Materials

The lignin was alkali lignin extracted from black liquor of papermaking (Shanhu Chemical, Nanjing, China), and its composition and structure are shown in Table S1 and S2, respectively. Ammonium borate (>98.9%, $(NH_4)_2B_4O_7{\cdot}4H_2O$) was purchased from Sigma-Aldrich.

The pretreatment method of lignin was as follows: 1g lignin and different amounts (0, 1%, 3% and 5%) of ammonium borate (BN) were added to 100 mL deionized water, and ultrasonic dispersion (40 kHz, 300 W) was performed at room temperature for 1 h. The mixed solution was then quickly dropped into liquid nitrogen for freezing. Finally, the frozen lignin particles were put into a vacuum freezing dryer and dried for 48h.

2.2. In situ analysis of lignin pyrolysis behavior

In situ ^{1}H NMR analysis was performed on a Bruker Avance III HD 300 MHz NMR instrument equipped with a Bruker SEI-HT high-temperature probe (Fig. S1). About 40 mg of lignin was put into an NMR quartz tube (5mm diameter), and then a glass capillary connected to high purity argon gas (10 ml/min) was inserted into the

tube to flush out the air. Then the quartz tube was put into the probe. The heating rate of the quartz tube was controlled at 5 ℃/min within the temperature range of 120~450 ℃. Solid echo experiments were recorded at intervals of 10 ℃ with a 128 scan accumulation and a recycle delay of 0.4 s. At each recording point, the probe was manually tuned to counteract temperature changes. MATLAB software was used to deconvolute the spectrum into a Gaussian peak (solid-like) and a Lorentzian peak (liquid-like), and the fitting regression coefficient (R^2) was always higher than 99% (examples are shown in Fig. S2) [6]. The fraction of mobile H protons in the fluid phase can be expressed by using Equation (1):

$$\%H_L = A_L/(A_L + A_G) \times 100\% \quad (1)$$

where A_L and A_G are the areas of Lorentzian and Gaussian peaks, respectively.

In situ rheological analysis of lignin was carried out in an ARES G2 high-torque controlled strain rheometer (Fig. S3). About 500 mg of lignin was pressed into pellets with a diameter of 10 mm and a height of about 4 mm. The sample was fixed between two parallel serrated plates, and a vertical static force of 200 g was applied. High purity N_2 was introduced into the furnace to provide an inert atmosphere, and the temperature increased from 90 ℃ to 450 ℃ at the heating rate of 5℃/min. Small amplitude of rotational oscillation was applied to the bottom plate with a strain amplitude of 1% and a frequency (ω) of 1 Hz (6.28 rad·s^{-1}). The oscillation of the bottom plate is transmitted through the sample to the upper plate, and its response is calculated to obtain the elastic modulus (G') and viscous modulus (G''). The complex viscosity (η^*) can be calculated from the Equation (2), and tan (δ) is given from the Equation (3):

$$|\eta^*| = \sqrt{(G'^2 + G''^2)}/\omega \quad (2)$$

$$\tan(\delta) = G''/G' \quad (3)$$

where δ ($0 < \delta < \pi/2$) is the phase angle between stress and strain. Where tan (δ) > 1, the material is mainly viscous, while tan (δ) < 1 depicts a mainly elastic material.

In situ DRIFT spectra of lignin pyrolysis were performed on a Bruker Vertex-70 FTIR spectrometer equipped with a diffuse reflectance accessory. Lignin was heated from 30 ℃ to 500 ℃ at a heating rate of 5 ℃/min. The spectra were recorded at 5 ℃ intervals with a resolution of 8 cm^{-1} and scanned 64 times per minute. Corresponding scans of pure KBr particles were taken as the background at each recording point. The relative intensity (I_v/I_m) of the functional group given is the ratio of the variable intensity (I_v) to the maximum intensity (I_m).

The slow pyrolysis experiment was carried out in a quartz U-shaped micro fixed bed reactor (length 25 mm, i.d. 10 mm) (**Fig. S4**). 200 mg lignin particles were pre-placed on the quartz sieve plate at the bottom of the reactor. N_2 was used as carrier gas with a flow rate of 200 mL /min. The furnace temperature was controlled by electric heating program, rising from 30 ℃ to 700 ℃ at a heating rate of 5 ℃/min. Thermocouples were inserted into the reactor to monitor the sample temperature. The volatiles were sampled through a quartz capillary transfer line (280 ℃) into SPI-TOFMS (Hefei University of Technology, China) for online analysis. The system is equipped with a VUV photoionization lamp module (PKS106, Heraeus, England) with a photon energy of 10.6 eV and a reflection TOF-MS with a mass resolution of 4000 [16].

3. Results and discussions

3.1. Evolution of mobile protons during lignin pyrolysis via in-situ ^{1}H NMR

The evolution of mobile protons during lignin pyrolysis is shown in **Fig. 1**. For raw lignin, the mobile H content increases gradually from 12% at 120 ℃ to 90% at 300 ℃, remains until 350 ℃, then rapidly decreases to 25% at 450 ℃. Specifically, at

120~300 ℃, the mobility of chain segments in lignin increases, and subsequent cleavage of bonds produces more fragments with higher fluidity[6]. The high fluidity at 300~350 ℃ might be related to the conversion of these fragments. While the rapid decay of mobile H after 350 ℃ might be due to the devolatilization (loss in H) and to crosslinking reactions [17].

With boron addition, the fraction of the fluid phase is reduced substantially. This demonstrates that the cross-linking between borates and lignin chains inhibits the formation of mobile H protons. With the increase of boron content, the maximum mobile proton content decreases. For 1%BN, two peaks (around 54%) of mobile protons appear at 250℃ and 350℃, respectively. The former might be related to the motion of chain segments or molecules inside the partly crosslinked structures, while the latter might be due to the depolymerization of chain segments to form a small number of mobile fragments. 3%BN and 5%BN also showed mobile protons peak with decreasing intensity to 41% and 32% around 250 ℃ respectively, which indicates that the mobility of chain segments becomes more difficult with the increase of crosslinking density. However, there is no peak that occurs around 350 ℃ for 3%BN and 5%BN, suggesting that the formation of mobile intermediates is considerably inhibited. It is worth noting that the fluidity of 5%BN lignin is lower than the reported fluidity of cellulose (35%) [6].

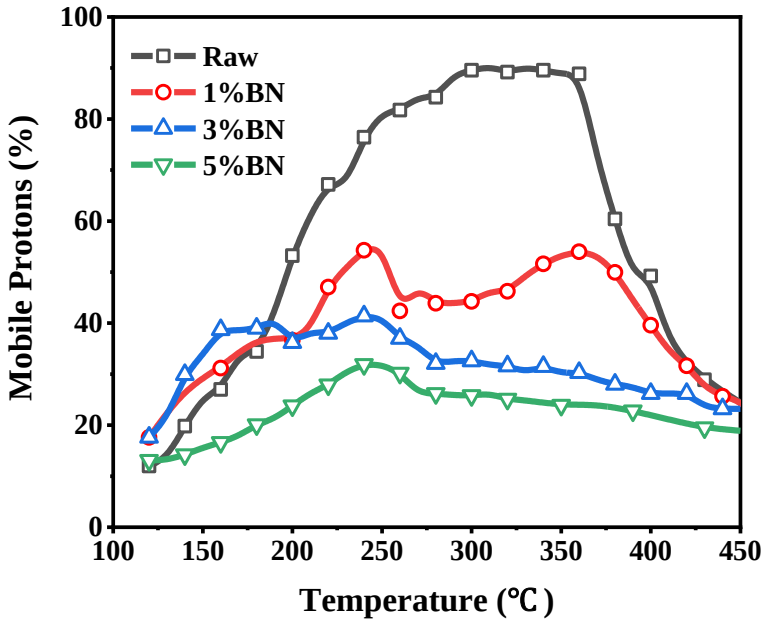

Fig.1. Evolution of mobile protons as a function of temperature

3.2. Evolution of viscoelastic properties during lignin pyrolysis via in-situ rheology analysis

Elastic (G') and viscous (G") moduli and deformation (displayed between 90 ℃ and 450 ℃) of lignin with boron addition are shown in **Fig. 2.** For raw lignin (**Fig. 2a**), the value of G' is higher than G" between 90 and 130 ℃, and there is no obvious deformation of lignin, indicating that lignin is mainly rigid at this temperature range. Then G' is equal to G" at 150 ℃ as a mark of the glass phase transition of lignin. Subsequently, lignin swells and then shrinks dramatically. The G' and G" values decrease, but the higher G" indicates that lignin has become mainly viscous. It is worth noting that with an increase of 30 ℃ (from 170 ℃ to 200 ℃), the deformation is as high as 60% (from +30% to -30%). From 200 °C, the G' value increases and is again above G", the matrix becomes mainly elastic and the deformation becomes stable. After 300 ℃, the G" value increases, indicating that the important crosslinking reactions happened leading to the resolidification of the matrix. As the temperature is higher than 380 °C, the value of G' (3 MPa) is much greater than that of G" (0.04

MPa). This highlights that the matrix becomes highly rigid, forming a brittle char. All these observations are consistent with our previous work on other lignins [3, 15].

With a low boron addition (1%BN), as shown in **Fig. 2b**, the glassy transition of lignin is delayed, and the swelling happens after 200 ℃. However, a deformation of 50% is reached, which is higher than that of the raw lignin (30%). At this point, both G' and G" decrease rapidly, confirming the breaking of interactions within the lignin matrix. Afterward, softening of the matrix occurs in a temperature range of 210~250 ℃. Both G' and G" remains stable and then increase, indicating that the interactions within the matrix are strengthened by crosslinking reactions.

With boron content increase (3%BN, **Fig. 2c**), the maximum deformation is around 40%, while the softening of lignin does not occur. Overall, the value of G' stays higher than G" and their difference remained constant, indicating that the matrix exhibits mainly elastic properties. It is interesting to note that the lignin exhibits two-step swelling at 150 ℃ and 230 ℃, respectively. Correspondingly, there are two "valleys" on the G' and G" curves. This implies that there might be two different interactions between borate and lignin, and the proposed interaction mechanism is shown in **Scheme 1**. The tetrahydroxy borate ($B(OH)_4^-$) produced by borate hydrolysis could either form non-covalent hydrogen bonds or undergo esterification to form borate esters with hydroxyl groups of lignin[12].

As shown in **Fig. 2d**, for 5%BN, no swelling and softening occur, while the slow linear deformation of the matrix is related to the thermal dilatation of the solid matrix. The initial values of G' and G" are reduced further compared to that of 3%BN.Both values remain stable with lower differences upon lignin thermal conversion.

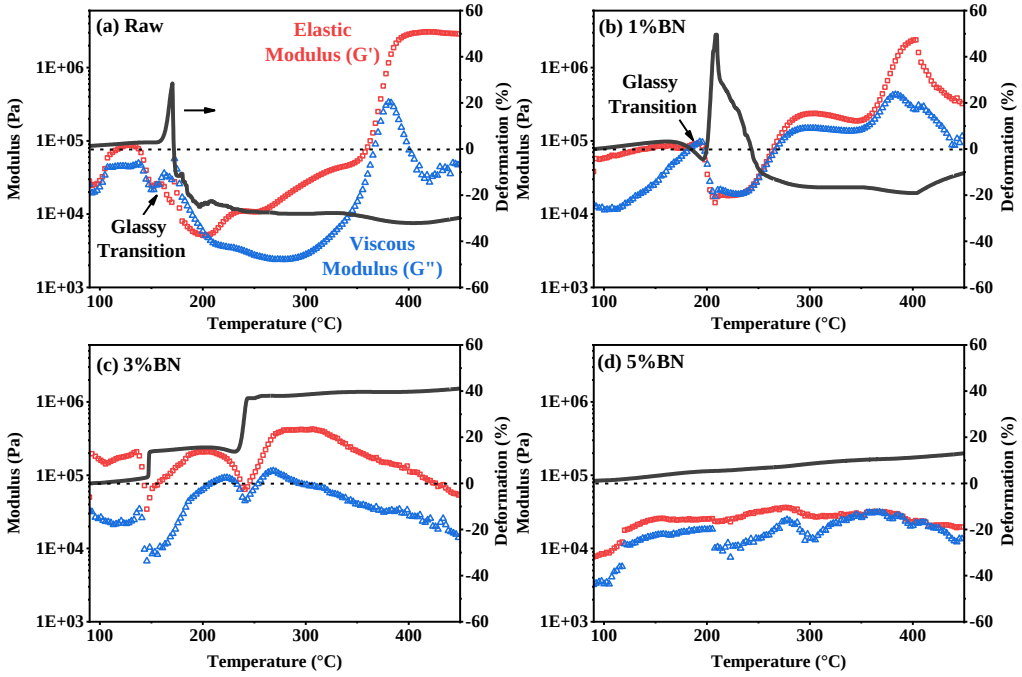

Fig. 2. The modulus and deformation curves of lignin samples measured via rheometer.

$$(NH_4)_2B_4O_7 + 7H_2O \rightarrow 4H_3BO_3 + 2NH_3\uparrow + 2H_2O \quad (1)$$

$$H_3BO_3 + 2H_2O \leftrightarrow [B(OH)_4]^- + H_3O^+ \quad (2)$$

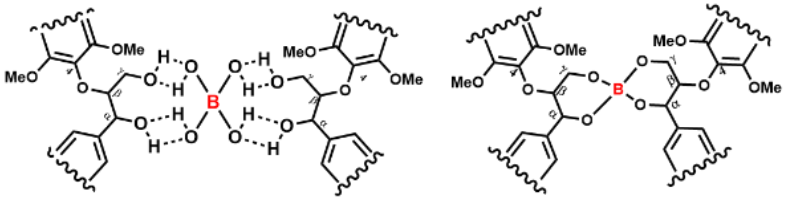

Scheme 1. Proposed interaction mechanism between borate and lignin chains during pretreatment.

The variation of tan (δ) reflects the evolution of the viscoelasticity of materials[3]. As shown in **Fig. 3**, the peak on the tan (δ) curve represents the tendency of lignin to change from solid to liquid. It can be seen that with the increase of boron amount, the transition peak (170 ℃) shifts to a higher temperature with the decreased intensity until it disappears completely (5%BN). This demonstrates the contribution of borates to the phase stability of lignin. The line of tan (δ) = 1 divided the curve into a

swelling-softening stage (tan (δ) > 1) and solidification stage (tan (δ) < 1). Both raw and 1%BN showed small peaks (350~400 ℃), which might be related to secondary cleavages of bonds (**Fig. 1**). Then the solidification of the matrix is accelerated with the release of volatiles, resulting in the formation of rigid char. Moreover, the peak intensity of the tan (δ) curve of 3%BN at 150 ℃ is lower than that at 200 ℃. The addition of boron provides a possible way to prepare high tensile strength lignin-based carbon fibers[18].

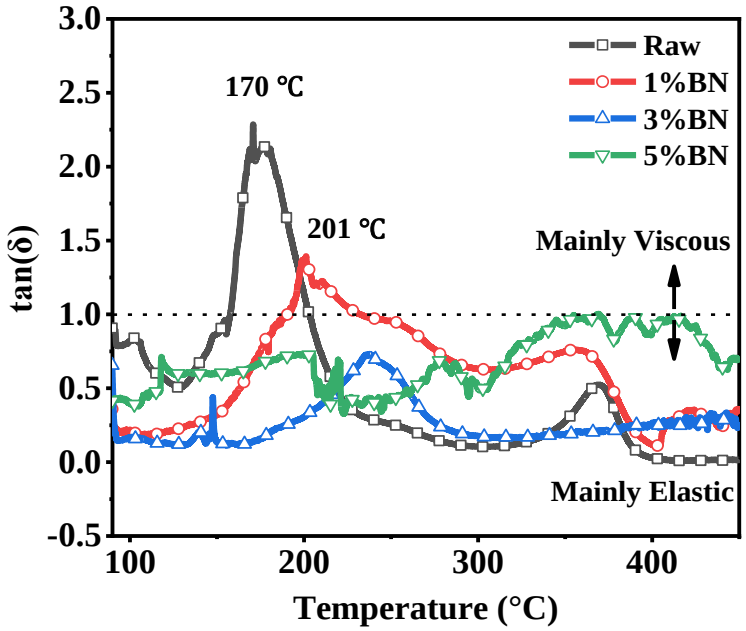

Fig. 3. Evolution of tan (δ) as a function of temperature.

3.3. Relation between mobile protons and complex viscosity during lignin pyrolysis

The relation between complex viscosity ($|\eta^*|$) and mobile protons is illustrated in **Fig. 4**. For raw lignin, both mobile protons (10%~90%) and $|\eta^*|$ value (7×10^3~3×10^6) vary over a wide range. At first, the value of $|\eta^*|$ decreases with the increase of mobile protons, corresponding to the softening stage. As the temperature rises to 210 ℃, the increase of the $|\eta^*|$ value indicates that the resolidification has started, although the

fluidity of protons still increases continuously. The decay of mobile protons might be caused by the high boiling-point liquid intermediates being entrapped in the solid "cavities"[19]. With the rearrangement, condensation, and crosslinking of the intermediates, the viscosity of the matrix increases rapidly to form a rigid char with still some mobile species present inside.

With boron addition, the evolution of mobile protons and complex viscosity is in a narrower range and both tend to shift to a lower value, as shown in **Fig. 4**. In particular, for 5%BN, few variations in $|\eta^*|$ value (2×10^4~4×10^4) with a lower fraction of fluid phase (10%~30%) is observed. This implies that the pre-crosslinking of borate promotes the formation of a stable rigid matrix upon lignin pyrolysis. Moreover, the decay of the mobile protons also improved with the increase of boron content, which might be related to the inhibited formation of liquid intermediates. This fundamentally explains why borate inhibits the formation of oligomers during lignin fast pyrolysis in our previous study, which is undoubtedly beneficial to improve the valorisation of bio-oil [20].

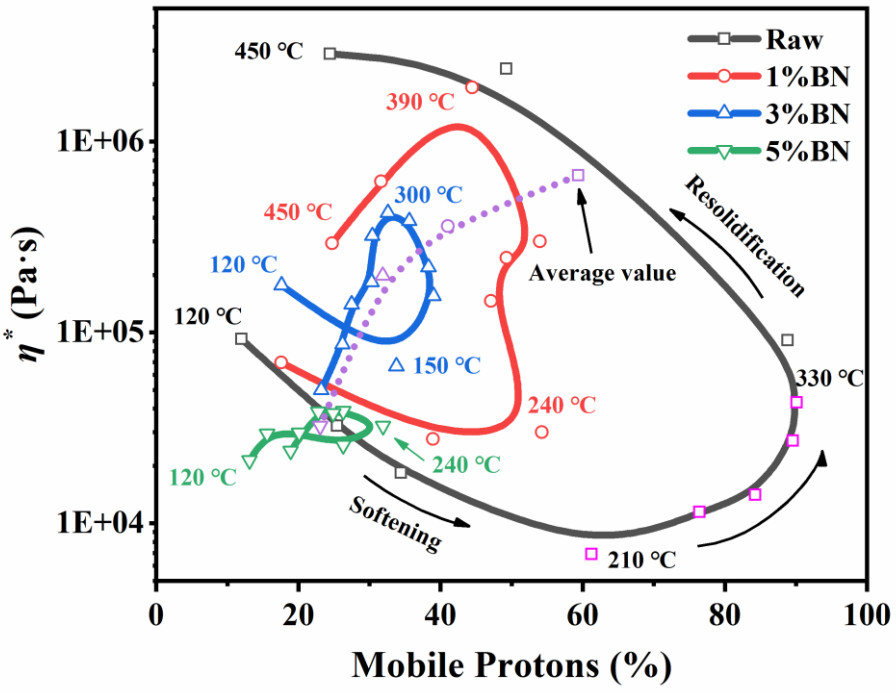

Fig. 4. Complex viscosity as a function of mobile protons during lignin pyrolysis.

3.4. Evolution of functional groups during pyrolysis via DRIFT spectroscopy

To better understand the impact of borate crosslinking on lignin functional groups during pyrolysis, *in situ* DRIFT spectroscopy was applied and the evolution of typical functional groups with temperature is shown in **Fig. 5**. The peak at 1125 cm^{-1} and 1210 cm^{-1} result from the vibration of C-O-C ether groups and the vibration of C-O in phenolic hydroxyl groups, respectively. The stretching of C=O in carboxyl or carbonyl groups appears at 1710 cm^{-1}, and the peaks at 1510 cm^{-1} and 1600 cm^{-1} are ascribed to the vibration of C-C in aromatic rings and the vibration of C=C in conjugated alkenes, respectively. In addition, a new peak was found at 1060 cm^{-1} caused by the vibration of C-O-B, which demonstrates the cross-linking of hydroxyl groups between borates and lignin.

For raw lignin, similarly, the intensity of ether bonds (**Fig. 5a**) and phenolic hydroxyl groups (**Fig. 5b**) decrease with the rise of temperature and tend to be stable after 400 ℃. With the addition of 1% and 3%BN, the decreases in phenolic and ether functional groups are not significantly affected. Nevertheless, as the additive content increases to 5%, more oxygenated groups remained in the biochar. This is in agreement with the characteristic of a low condensation degree of residual char (**Fig. 2d**). Coincidentally, shoulders around 150 ℃ and 200 ℃ are observed on the curves of functional groups of raw and 1%BN lignin, respectively, corresponding to their respective softening stages (**Fig. 2a** and **2b**).

The variation curves of carbonyl (**Fig. 5c**) and conjugated olefin (**Fig. 5d**) are similar. Their content does not decrease but increases from 200 ℃, and decreases rapidly after reaching the maximum at 300 ℃. These groups might be formed by dehydration or concerted reactions of aryl side chains[22]. With the addition of boron, the formation of

carbonyl and conjugated olefin are delayed or inhibited, particularly for 5%BN, which is predominantly related to the shielding of reactive hydroxyl groups in lignin. This is also illustrated by the decay of mobile H content (**Fig. 1**). As evidence, the decrease of C-O-B before 200 ℃ indicates the destruction of the borate ester structures (**Fig. 5e**), while the subsequent increase might be related to the formation of the new BCO structures in biochar[13]. These BCO structures have a strong anchoring effect on oxygen and carbon atoms, which enhance the surface polarity, and are considered to be the main active sites of biochar for catalysis and adsorption[23].

As mentioned earlier, except to form covalent borate ester, there is also hydrogen bonding between borate and lignin, which has a great effect on the thermal mobility of lignin[7]. The intensity ratio between intermolecular (3200 cm^{-1}) and intramolecular (3520 cm^{-1}) hydrogen bonds is shown in **Fig. 5f**. For raw lignin, the relative intensity of hydrogen bonds decreases with the increase of temperature (below 220 ℃), suggesting that the cleavage of intermolecular hydrogen bonds is faster during the lignin swelling and softening process. Subsequently, the relative intensity of hydrogen bonds increased rapidly until 330 ℃, indicating that the breaking of intramolecular hydrogen bonds is dominant. This might be caused by dehydration, depolymerization, and condensation during lignin pyrolysis, which is associated with the second peak of tan (δ) in **Fig. 3**. As the temperature continues to rise, the intensity of the two hydrogen bonds tends to balance, since the amount of hydrogen bonds in the rigid matrix is close to zero.

With boron addition, the evolution of hydrogen bonds with temperature is similar to that of raw lignin. However, with the increase of boron amount, the fluctuation range of the relative intensity decreases, especially the peak within 300~400 ℃ becomes weak, indicating that the conversion of intramolecular hydrogen bonds is inhibited.

Besides, the impact of borate at lower content on hydrogen bond before 220 ℃ seems weak. This suggests that covalent borate ester (C-O-B) is the dominant binding form of borate and lignin. While for 5%BN, the initial relative intensity of hydrogen bond increased obviously, confirming the formation of new intermolecular hydrogen bonds between borate and lignin hydroxyls (**Scheme 1**).

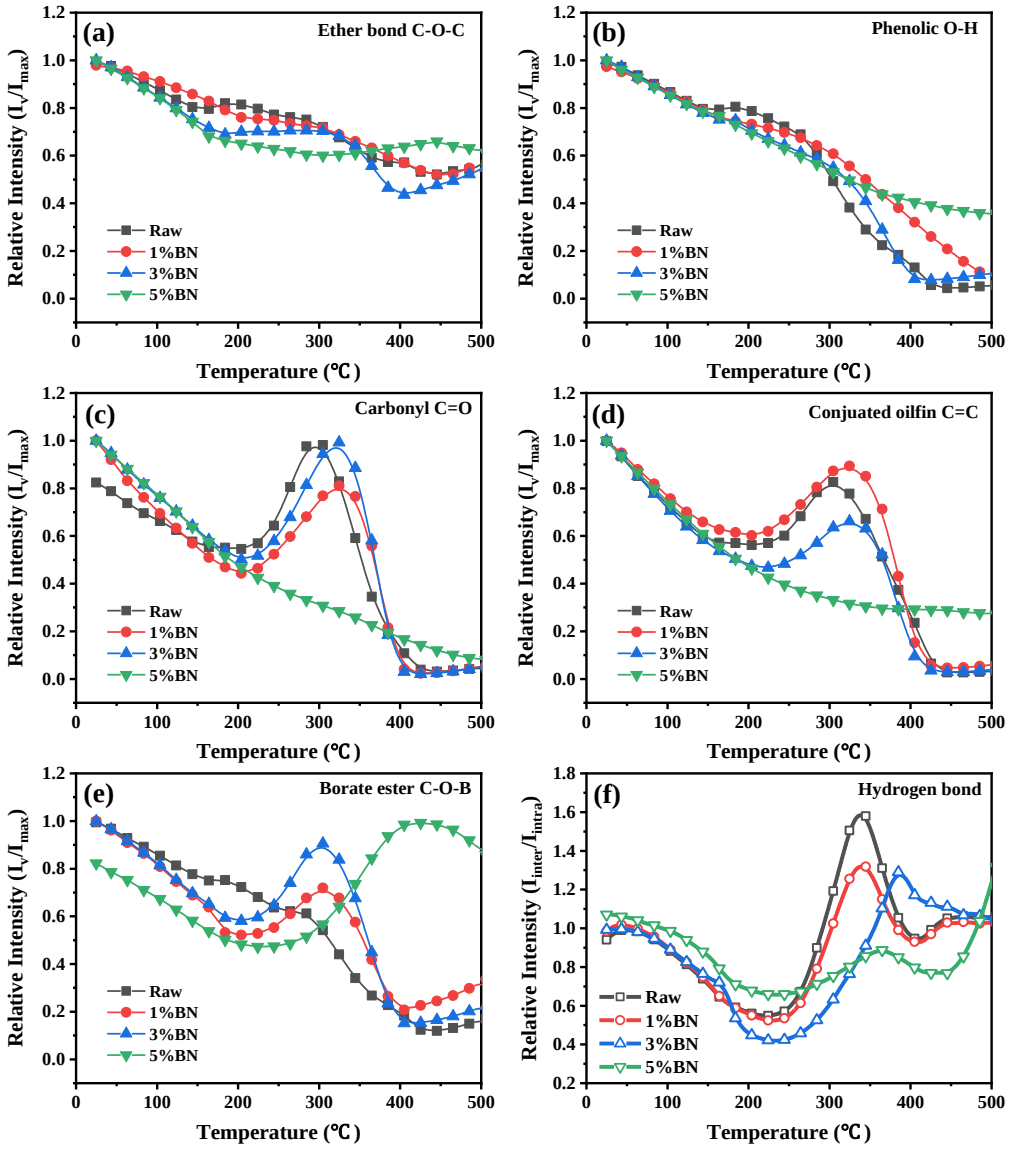

Fig. 5. (a-e) Evolution of functional groups; (f) Relative intensity of intermolecular and intramolecular hydrogen bonds as a function of temperature

3.5. Online analysis of volatiles during lignin pyrolysis via SPI-MS

The release of volatiles from lignin slow pyrolysis in a microreactor was online

monitored using SPI-MS. The cumulative content of the main vapor products is shown in **Table S4**. Guaiacol (m/z = 124), 4-methyl guaiacol (m/z = 138), catechol (m/z = 110) and 4-vinyl guaiacol (m/z = 150) are the main products, and more vanillin (m/z = 152) and eugenol (m/z = 164) has also been detected. With boron addition, the content of phenol (m/z = 94), cresol (m/z = 108), catechol, guaiacol and vanillin increases, reaching a maximum for 3%BN. This suggests that the introduction of boron may be advantageous for the formation of simple phenols. However, as boron content increases to 5%BN, the type and yield of volatile products are reduced, which is consistent with the evolution of functional groups in the solid matrix (**Fig. 5**).

The evolution of typical volatiles during pyrolysis is shown in **Fig. 6**. For raw lignin (**Fig. 6a**), the release profile of volatiles can be divided into two stages: 150 ℃ ~ 250 ℃ and 250 ℃ ~ 550 ℃, which correspond to the softening and solidification stages of lignin, respectively (**Fig. 2a**). The smaller first release peak around 180 ℃ (including guaiacol, vanillin, and 4-propyl guaiacol) may be formed by desorption of free compounds or by the cleavage of weak bonds (like ether ones) . The larger second peak near 400 °C is due to the important depolymerization reactions. In the second stage, it can be seen that the release sequence of the compounds is: 4-vinyl phenol and eugenol < guaiacol, 4-methyl guaiacol < vanillin and 4-propyl guaiacol < catechol. When volatiles are largely released (400 ℃), the mobile protons also decrease (**Fig. 1**). Therefore, light volatiles may come from the secondary reactions of the mobile intermediates (like oligomers present in the liquid state at 300-400°C) [1].

For 1%BN (**Fig. 6b**) and 3%BN (**Fig. 6c**), compare with raw lignin, there was no significant change in the peak position of the products, while the signals of guaiacol derivatives, such as 4-vinyl guaiacol, 4-methyl guaiacol, and eugenol, are significantly attenuated. This might be because the crosslinking of borates to

side-chain hydroxyl groups inhibits the fracture of linkages between phenylpropane units. However, for 5% BN (**Fig. 6d**), the release peak temperatures of the volatiles decrease. This is consistent with the TGA results of our previous study [20], that higher crosslinking density leads to a forward shift of the mass loss rate peak. Furthermore, different from the raw lignin, the volatiles are rather produced from the pyrolysis of the rigid lignin-borate network due to the reduction in mobile intermediates.

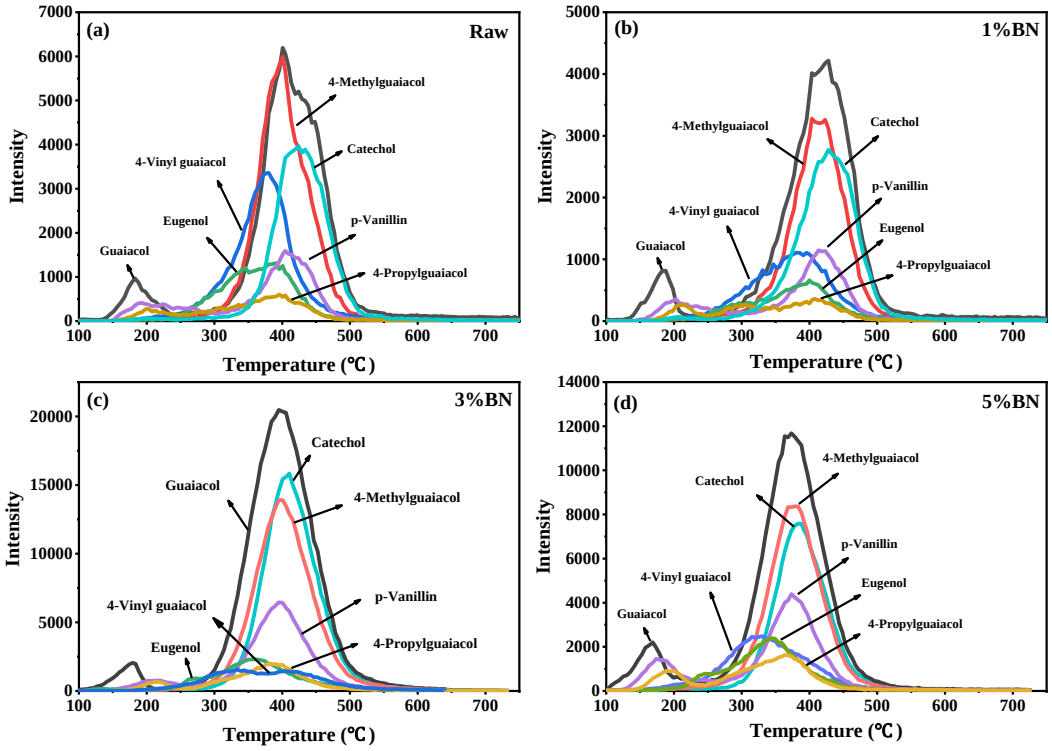

Fig. 6. Release profile of typical volatiles during lignin pyrolysis

3.6. Physical-chemical mechanism of borate modified lignin pyrolysis

A possible pyrolysis mechanism of raw and borate modified lignin is proposed in **Scheme 2**. For raw lignin, the amorphous lignin chains become mobile at 150 ℃, and then the slippage of chains starts from 170 ℃ due to the poor interactions of lignin molecules[25]. This corresponds to the swelling and softening of the matrix as analyzed at the macroscopic scale by in-situ rheology. Subsequently, the aryl ether

bonds, such as β-O-4, are cleaved as evidenced by in-situ DRIFT, resulting in the depolymerization of the lignin chain into free radical fragments with higher mobility. These intermediates are further cracked to form vapor products, or crosslinked and repolymerized to form solid char. The crosslinking of the viscous matrix entraps mobile intermediates (as analyzed by in-situ NMR) in rigid "cavities". This mechanism impedes the release of volatiles and promotes the secondary reactions of mobile species entrapped in the cavities.

The pretreatment with borate considerably impacts the mechanisms of lignin pyrolysis. Borate and lignin form a crosslinked network through hydrogen bonds and C-O-B bonds, which inhibit the mobility of lignin chains. The cleavage of bonds mainly occurs in a rigid matrix with less mobile transferable protons. The new BCO structure is formed in the char as evidenced by DRIFT spectra, which is consistent with our previous analysis of boron-doped char[13]. The boron-doped char presents an increased oxygen-grafting and interesting electronic properties of potential interest for high added-value applications [26].

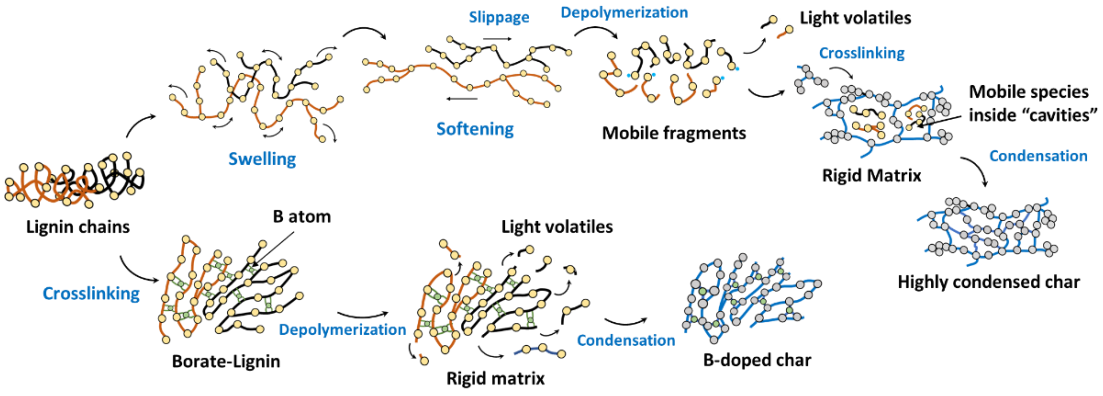

Scheme 2. Proposed evolution mechanism of lignin chains during pyrolysis

4. Conclusions

This study investigates the mechanism of borate crosslinking on lignin softening and pyrolysis process by in situ physical and chemical techniques. The physical states

of lignin undergo glassy transition, swelling, softening, and resolidification stages. For raw lignin, the mobile protons become up to 90%. The interactions formed between borate and lignin include hydrogen bonding and crosslinked borate ester, the latter being dominant. With the increase of boron content, the content of mobile protons decreases, and the matrix stays mainly rigid with low deformation (lowered swelling and shrinking). The pre-crosslinking by borate inhibits lignin softening and foaming. In addition, the shielding of lignin hydroxyl groups by borate inhibits the decomposition of lignin but improves the selectivity of simple phenols, and more oxygenic groups remain in the solid char.

Acknowledgements

The authors gratefully acknowledge the financial support of the National Nature Science Foundation of China (51976065), China Postdoctoral Science Foundation (2018M640696 and 2019T120664) and China Scholarship Council, and the technical support from the Analytical and Testing Center in Huazhong University of Science & Technology (http://atc.hust.edu.cn).

Supplementary materials

Supplementary material associated with this article can be found in the online version.

References:

[1] E. Terrell, L.D. Dellon, A. Dufour, E. Bartolomei, L.J. Broadbelt, M. Garcia-Perez, A Review on Lignin Liquefaction: Advanced Characterization of Structure and Microkinetic Modeling, Ind. Eng. Chem., 59 (2019) 526-555.

[2] S. Zhou, R.C. Brown, X. Bai, The use of calcium hydroxide pretreatment to overcome agglomeration of technical lignin during fast pyrolysis, Green Chem., 17 (2015) 4748-4759.

399 [3] B. Shrestha, Y. le Brech, T. Ghislain, S. Leclerc, V. Carré, F. Aubriet, S. Hoppe, P.
400 Marchal, S. Pontvianne, N. Brosse, A. Dufour, A Multitechnique Characterization of
401 Lignin Softening and Pyrolysis, ACS Sustain. Chem. Eng., 5 (2017) 6940-6949.
402 [4] J.A. Tiarks, C.E. Dedic, T.R. Meyer, R.C. Brown, J.B. Michael, Visualization of
403 physicochemical phenomena during biomass pyrolysis in an optically accessible
404 reactor, J. Anal. Appl. Pyrolysis, 143 (2019) 104667.
405 [5] S. Zhou, B. Pecha, M. van Kuppevelt, A.G. McDonald, M. Garcia-Perez, Slow and
406 fast pyrolysis of Douglas-fir lignin: Importance of liquid-intermediate formation on the
407 distribution of products, Biomass Bioenergy, 66 (2014) 398-409.
408 [6] A. Dufour, M. Castro-Diaz, N. Brosse, M. Bouroukba, C. Snape, The origin of
409 molecular mobility during biomass pyrolysis as revealed by in situ (1)H NMR
410 spectroscopy, ChemSusChem, 5 (2012) 1258-1265.
411 [7] S. Kubo, J.F. Kadla, Hydrogen bonding in lignin: a Fourier transform infrared
412 model compound study, Biomacromolecules, 6 (2005) 2815-2821.
413 [8] X. Xin, K.M. Torr, F. de Miguel Mercader, S. Pang, Insights into Preventing
414 Fluidized Bed Material Agglomeration in Fast Pyrolysis of Acid-Leached Pine Wood,
415 Energy Fuels, 33 (2019) 4254-4263.
416 [9] B.D. Stef Ghysels, Jan Van den Bulcke, Hero Jan Heeres; Mehmet Pala, Léon
417 Rohrbach, and Frederik Ronsse, Improving fast pyrolysis of lignin using three additives
418 with different modes of action, Green Chem., 22 (2020) 6471-6488.
419 [10] J. Li, X. Bai, Z. Dong, Y. Chen, H. Yang, X. Wang, H.J.F. Chen, Influence of
420 additives on lignin agglomeration and pyrolysis behavior, Fuel, 263 (2020) 116629.
421 [11] H.W. Lee, Y.-M. Kim, J. Jae, S.M. Lee, S.-C. Jung, Y.-K. Park, The use of calcined
422 seashell for the prevention of char foaming/agglomeration and the production of
423 high-quality oil during the pyrolysis of lignin, Renewable Energy, 144 (2019) 147-152.

[12] N.-D. Le, M. Trogen, R.J. Varley, M. Hummel, N. Byrne, Effect of boric acid on the stabilisation of cellulose-lignin filaments as precursors for carbon fibres, Cellulose, 28 (2020) 729-739.

[13] Z. Dong, H. Yang, Z. Liu, P. Chen, Y. Chen, X. Wang, H.J.F. Chen, Effect of boron-based additives on char agglomeration and boron doped carbon microspheres structure from lignin pyrolysis, Fuel, 303 (2021) 121237.

[14] G. Dai, G. Wang, K. Wang, Z. Zhou, S. Wang, Mechanism study of hemicellulose pyrolysis by combining in-situ DRIFT, TGA-PIMS and theoretical calculation, Proc. Combust. Inst., 38 (2021) 4241-4249.

[15] A. Dufour, M. Castro-Díaz, P. Marchal, N. Brosse, R. Olcese, M. Bouroukba, C. Snape, In Situ Analysis of Biomass Pyrolysis by High Temperature Rheology in Relations with 1H NMR, Energy Fuels, 26 (2012) 6432-6441.

[16] L. Chen, K. Yang, J. Huang, P. Liu, J. Yang, Y. Pan, F. Qi, L. Jia, Experimental and kinetic study on flash pyrolysis of biomass via on-line photoionization mass spectrometry, Applications in Energy and Combustion Science, 9 (2022).

[17] B. Hu, W. Xie, Y. Li, Z. Zhang, J. Liu, B. Zhang, T. Wang, Q. Lu, Hydroxyl-Assisted Hydrogen Transfer Interaction in Lignin Pyrolysis: An Extended Concerted Interaction Mechanism, Energy Fuels, 35 (2021) 13170-13180.

[18] W. Qu, J. Yang, X. Sun, X. Bai, H. Jin, M. Zhang, Towards producing high-quality lignin-based carbon fibers: A review of crucial factors affecting lignin properties and conversion techniques, Int J Biol Macromol, 189 (2021) 768-784.

[19] V. Mamleev, S. Bourbigot, M. Le Bras, J. Yvon, The facts and hypotheses relating to the phenomenological model of cellulose pyrolysis, J. Anal. Appl. Pyrolysis, 84 (2009) 1-17.

[20] Z. Dong, H. Yang, Z. Liu, P. Chen, Y. Chen, X. Wang, H. Chen, S. Wang, Pyrolysis

449 of boron-crosslinked lignin: influence on lignin softening and product properties,
450 Bioresour Technol, (2022) 127218.
451 [21] J.-P.G. P. S. Thomas, G. F. Russell and B. J. Briscoe, FTIR study of the thermal
452 degradation of poly (vinyl alcohol), J. Therm. Anal. Calorim., 64 (2001) 501-508.
453 [22] G. Dai, K. Wang, G. Wang, S. Wang, Initial pyrolysis mechanism of cellulose
454 revealed by in-situ DRIFT analysis and theoretical calculation, Combust. Flame, 208
455 (2019) 273-280.
456 [23] Y. Wang, M. Liu, X. Zhao, D. Cao, T. Guo, B. Yang, Insights into heterogeneous
457 catalysis of peroxymonosulfate activation by boron-doped ordered mesoporous carbon,
458 Carbon, 135 (2018) 238-247.
459 [24] C. Liu, Y. Deng, S. Wu, H. Mou, J. Liang, M. Lei, Study on the pyrolysis
460 mechanism of three guaiacyl-type lignin monomeric model compounds, J. Anal. Appl.
461 Pyrolysis, 118 (2016) 123-129.
462 [25] L. Wei, U.P. Agarwal, L. Matuana, R.C. Sabo, N.M. Stark, Performance of high
463 lignin content cellulose nanocrystals in poly(lactic acid), Polymer, 135 (2018) 305-313.
464 [26] F. Sun, Z. Qu, J. Gao, H.B. Wu, F. Liu, R. Han, L. Wang, T. Pei, G. Zhao, Y. Lu, In
465 Situ Doping Boron Atoms into Porous Carbon Nanoparticles with Increased Oxygen
466 Graft Enhances both Affinity and Durability toward Electrolyte for Greatly Improved
467 Supercapacitive Performance, Adv. Funct. Mater., 28 (2018) 1804190.
468